The effect of “Fishery-PV Integration” on Penaeus monodon culture and Micro-ecological environment

Chengbo Sun (suncb@gdou.edu.cn)
Guangdong Ocean University
Minze Liao
Guangdong Ocean University
Xinxin Long
Guangdong Ocean University
Zihao He
Guangdong Ocean University
Jichen Zhao
Guangdong Ocean University
Xieyan Chen
Guangdong Ocean University
Dongwenjun Zhu
Guangdong Ocean University

Research Article

Keywords: Fishery-PV Integration, microbial community, antibiotic resistance genes, Penaeus monodon, metagenomics, 16S rRNA gene se

Posted Date: April 13th, 2022

DOI: https://doi.org/10.21203/rs.3.rs-1541781/v1

The effect of "Fishery-PV Integration" on *Penaeus monodon* culture and Micro-ecological environment

Minze Liao[1†], Xinxin Long[1†], Zihao He[1], Jichen Zhao[1], Xieyan Chen[1], Dongwenjun Zhu[1], Chengbo Sun[1, 2, 3*]

Abstract

Background: "Fishery-photovoltaic (PV) Integration" is a novel aquaculture model which aims to combine green energy with modern fisheries to improve socioeconomic benefits while ensuring aquaculture production and electricity consumption. To determine the practicability of the "Fishery-PV Integration" model, an experiment was conducted with *Penaeus monodon* as a model, in which the growth rates of shrimp, water quality conditions, and the micro-ecological environment were studied.

Results: After 105 days of rearing, *P. monodon* (initial weight of 0.006 ± 0.001 g) reached an average body weight of 11.69 ± 0.92 g. The water quality was stable ($C(NH_4^+) \leq 1.57$ mg/L), and the shrimps were healthy. It was determined via metagenomics and 16S rRNA gene sequencing that the dominant phyla present in shrimp intestines, water, and effluent were Proteobacteria, Actinobacteriota, Bacteroidota, and Verrucomicrobiota. In addition, a large number of nitrogen-fixing bacteria in the "Fishery-PV Integration" pond, which were helpful to maintain the stability of the water quality. The relative abundance of *Vibrio* as a common opportunistic pathogen for shrimp was relatively low, which is beneficial to promote the healthy growth of shrimp. In addition to maintaining water quality stability, microorganisms played an essential role in regulating intestinal amino acid metabolism, carbohydrate metabolism, and energy

metabolism. In the water and effluent, a high proportion of ABC transporters and quorum sensing play an important role in mitigating environmental toxins and regulating the physiological and metabolic activities of microbial communities. Notably, only 123 antibiotic resistance genes (ARGs) were identified within the “Fishery-PV Integration” pond. This result is significantly lower than the numbers found in other studies, indicating that shrimp cultured in the “Fishery-PV Integration” pond had a higher level of food safety.

Conclusions: This paper was the first reported the “Fishery-PV Integration” culture mode and preliminarily reveal the characteristics of the microflora and ARGs distribution in a “Fishery-PV Integration” pond. The results show that “Fishery-PV Integration” farming is a sustainable, green, and safe culture method.

Keywords: Fishery-PV Integration; microbial community; antibiotic resistance genes; *Penaeus monodon*; metagenomics; 16S rRNA gene sequencing

1. Introduction

With the rapid depletion of global fossil energy sources and the continuous emission of carbon dioxide, humanity must now reckon with energy shortages and the warming of the planet (Valipour, 2012; Yannopoulos, et al., 2015). As such, the demand for and importance of alternative energy sources has become evident. Solar photovoltaic (PV) power generation is a clean and promising renewable energy technology with the potential to replace traditional fossil fuels (Bazilian, et al., 2013). In recent years, with the strong support of governments around the world, methods of PV power generation have gradually diversified. Ranging from PV power stations built in the desert (Yuan, 2020) to solar panels installed on a grassland (Armstrong, et al., 2016), PV power generation is highly adaptable. In addition to being built on land, PV power stations can also be built on the

water. A recent study showed that laying PV panels on water can reduce evaporation (Trapani, et al., 2015). In addition, PV panels installed on water display improved conversion efficiency due to water's cooling effects (Bahaidarah, et al., 2013). PV panels on water can withstand typhoons, meaning that cultured organisms have a quiet growth environment and reduced losses due to natural disasters. Li et al. (2020b) studied the effects of different proportions of PV panels on water and fish, with results showing that the PV layout had no impact on the growth of fish, which somewhat confirms the safety of this farming mode. The Chinese government is striving to achieve "carbon neutral" status by 2060. However, reducing carbon dioxide emissions and developing renewable energy is a challenging task. A fish-lighting complementary PV power station organically combines aquaculture and renewable energy (Li, et al., 2020b). This setup combines overwater power generation and underwater aquaculture, which not only meets carbon emissions requirements but also provides a solution for energy demands. As such, it achieves a double harvest of fishing and electricity. The fish-lighting complementary PV power mode is aligned with the concept of green development. Furthermore, research has shown that the integration of aquaculture and solar power generation can improve the economic efficiency and employment level of aquaculture systems (Dong, et al., 2022), and play an important role in aquaculture's ability to resolve energy demands (Li, et al., 2020b). Consequently, the "Fishery-PV Integration" mode has broad developmental prospects.

With the continuous reduction of global fishery resources, aquaculture will play an increasingly important role in the supply of human seafood (Huang, et al., 2018a). Shrimp farming is a vital component of aquaculture. The giant tiger prawn, *P. monodon*, is one of the most economically important aquaculture shrimps in coastal China. It is widely cultured around the world

because of its rapid growth rate and strong disease resistance (Nguyen, et al., 2020). However, as high-density farms become mainstream, the environmental conditions of aquaculture waters are deteriorating, resulting in shrimp aquaculture diseases becoming especially common.

Bacterial diseases caused by the homeostatic imbalance of microbial communities in ecosystems have restricted the continued growth of shrimp aquaculture. Diseases caused by pathogenic bacteria—such as hepatopancreas necrosis syndrome (HPNS), early mortality syndrome (EMS) and acute hepatopancreatic necrosis disease (AHPND)—have caused tremendous harm to shrimp culture (Flegel, 2012). As a result, there is an urgent need to establish reliable strategies to prevent the incidence of shrimp disease. In an aquaculture ecosystem, aquatic animals interact directly with environmental microbial communities in which beneficial microorganisms play a crucial role in material circulation, water quality regulation, and host health (Blancheton, et al., 2013; Giatsis, et al., 2015). On the other hand, infection by pathogenic microbes can disrupt the dynamic balance of the host's intestinal environment and reduce the amount of potentially beneficial bacteria while increasing the amount of harmful bacteria, leading to the occurrence of disease (Huang, et al., 2020; Wma, et al., 2020). Indeed, the diseases affecting shrimp are strongly associated with the composition of the microorganism load in surrounding waters (Wang, et al., 2020; Zhang, et al., 2020) found that pond microbial communities in diseased shrimp populations were markedly distinct from those of healthy shrimp populations, and proposed that the composition of a bacterioplankton community can be used as a biological indicator to assess which shrimp diseases may occur (Wma, et al., 2020). Furthermore, Lucas et al. (2010) argue that microbial loops are dominant in the water column food web, and state that when a large amount of nutrients are suddenly imported, the microbial cycle function would be altered and the abundance of harmful

bacteria would increase, leading to the outbreak of bacterial disease in shrimp. For this reason, studying a water body's microbial composition and its relationship to shrimp intestinal and surrounding bacteria loads is important for the prevention and control of shrimp disease. Antibiotics have long been used in aquaculture to prevent diseases and promote shrimp growth. Nevertheless, the spread of antibiotic resistance genes (ARGs) in aquatic products has raised concerns due to the overuse of antibiotics in aquaculture (Abriouel, et al., 2008). As emerging environmental contaminants, ARGs had numerous adverse effects on the ecological environment and human health (Pruden, et al., 2006). Consuming fishery products contaminated with antibiotics may cause adverse drug reactions or antibiotic-resistant bacteria in humans (Liu, et al., 2017). Thus, as a new aquaculture mode, it is necessary to scientifically evaluate the ARGs of cultured animals and their surroundings in a "Fishery-PV Integration" pond.

In recent years, aquaculture has developed rapidly, but its level of intensification is low and mainly based on extensive farming (Dong, et al., 2022). One important reason is that intelligent fishery facilities and equipment consume a large amount of electricity, which increases the cost of farming. "Fishery-PV Integration" seeks to solve this problem and promote the modernization of fisheries. In addition, PV panels can provide power to cold chain logistics warehouses, thus promoting the development of fisheries. Currently, amplicon and metagenomic sequencing have been widely applied to study the microflora of aquaculture environments, including traditional white shrimp ponds (Zhang, et al., 2019), higher-place white shrimp ponds (He, et al., 2020), and biofloc-based aquaculture ponds (Chen, et al., 2022), etc. Therefore, to explore the practicability of the "Fishery-PV Integration" farming model, the present study cultured *P. monodon* in the "Fishery-PV Integration" engineering culture system and used metagenomic sequencing and 16S

rRNA gene sequencing technologies to compare the composition, function, and ARGs profiles of bacterial communities in shrimp intestines, water, and effluent. It aims to provide a scientific basis and supportive data for the large-scale application of PV in aquaculture and contribute to the adoption of the "Fishery-PV Integration" cultivation mode.

2. Material and methods

2.1 Composition of "Fishery-PV Integration" culture system

The shrimp "Fishery-PV Integration" culture system consists of a plastic film pond culture system and PV system (Fig. 1). The plastic film pond culture system consists of four parts: a culture pond with plastic film, an oxygen enrichment system, an influent and effluent system, and a tail water treatment system. The area of the plastic film pond used in this study was 300-600 m^2, with a depth of 1.5 m at the pond edge; the pond dike was 50 cm above the ground, and the bottom of the pond was the shape of a pot with a slope of 45°. In addition, the center of the pond had a sewage outfall with a diameter of 16 cm and a plastic film with a thickness of 0.1 cm was laid on the bottom and slope of the pond. The oxygen enrichment system was composed of a micro-porous aeration disc, oxygen pipeline, and blower. The density of the aeration disc in the pond was 1 / 10 m^2. The influent and effluent system consisted of a pump, a water supply pipe, and a drainpipe. The tail water treatment system used a three-stage aquaculture treatment system: (1) the primary treatment was conducted by herbivorous and omnivorous fish feeding on large particles, feed residues, and excrement in tail water; (2) the secondary treatment system relied on filter-feeding shellfish to remove suspended matter; and (3) the tertiary treatment was an algae-water purification system. The

PV system consisted of PV panels and columns. The maximum and minimum heights of the PV panels were 2.5 m and 2.2 m, and the light transmittance was 30%.

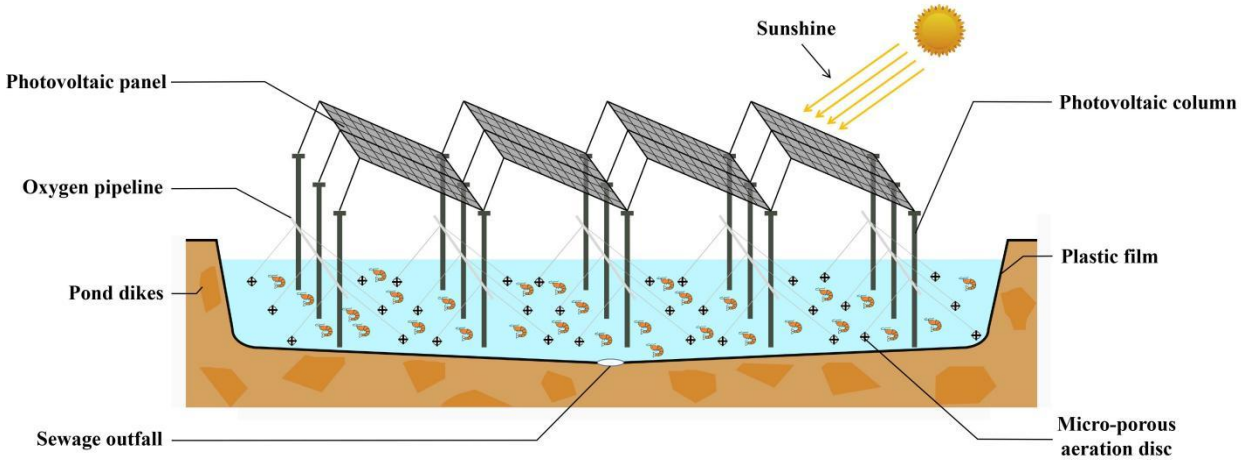

Fig. 1. Schematic diagram of "Fishery-PV Integration" culture pond.

2.2 Shrimp rearing and sample collection

The culture experiment was conducted at Xinrun Aquaculture Co. Ltd. in Fangchenggang city, Guangxi Province, China. Healthy juvenile *P. monodon* were purchased from a culture farm on Donghai Island in Zhanjiang (Guangdong, China). They were transferred into three "Fishery-PV Integration" ponds (J1, J2, J3) for rearing at a stocking density of 150 individuals/m^2. During the rearing period, the amount of the following day's feed was determined by the food intake of the shrimp on the previous day. The shrimps were fed with equal amounts of a commercial diet four times daily (7:00, 11:00, 18:00 and 23:00). Ammonia nitrogen, nitrite, and nitrate levels were chemically detected after 15 days, and every 5 days following (Lei, 2006). In addition, the body length and weight of the *P. monodon* were measured every 15 days. No diseases occurred and no fishery drugs were used throughout the experimental period.

At the end of the rearing period, water, effluent, and healthy shrimp intestine samples were collected from the each of the "Fishery-PV Integration" ponds. Water samples were collected at a

depth of 50 cm below the water surface using a multi-point sampling method (four diagonals and the central area of the pond), following which same-pond samples were combined and labelled JW1, JW2, and JW3, respectively. Meanwhile, effluent samples were also collected from three ponds with a corer sampler and labelled JT1, JT2, and JT3. Approximately 30 healthy shrimp (no disease characteristics) were taken from each pond and subjected to intestinal microbiota analysis. The sampled shrimp had an average body length of 10.69 ± 0.66 cm. Intestinal sampling was conducted according to previously reported methods (Rungrassamee, et al., 2016): after the shrimp bodies were washed with water and 75% ethanol, the intestines were stripped with sterilizing tools. Then, the intestinal contents of the shrimp from each pond were collected in a 10 ml centrifuge tube and labeled JI1, JI2, and JI3, respectively. All samples were stored at -80°C until DNA extraction.

2.3 Microbial DNA extraction

Total genomic DNA of the shrimp intestines, water, and effluent were extracted with TIANamp Soil DNA Kit (TIANGEN, Beijing, China) following the manufacturer's protocol. 1 L of water or effluent samples were filtered through 0.22 μm millipore filter membranes to collect microorganisms (Jinteng, Tianjin, China), which were aseptically cut into quarters for DNA extraction. Shrimp gut samples were directly used for DNA extraction. DNA concentration and purity were measured using a NanoVuePlus Spectrophotometer (GE Healthcare, Illinois, United States). The quality of the total DNA was monitored on 1% agARGsse gels. After quality assessment, DNA was stored at −80 °C until use.

2.4 16S rRNA gene amplification and pyrosequencing

For further analysis of the microbial community, nine prepared DNA samples from water, effluent, and intestinal contents were sent to Novogene Biological Information Technology Co.

(Tianjin, China). The specific primer pair 515F (5′-GTGCCAGCMGCCGCGGTAA-3′) and 806R (5′-GGACTACHVGGGTWTCTAAT-3′) was applied to amplify the V3-V4 hypervariable region of the 16S rRNA gene, which carries a unique barcode to distinguish samples. All PCR reactions were carried out using a 15 μL of Phusion® High-Fidelity PCR Master Mix (New England Biolabs, Massachusetts, United States). PCR was performed at 98℃ for 1 min, followed by 30 cycles at 98℃ for 10 s, at 50℃ for 30 s, and at 72℃ for 30 s, ending at 72℃ for 5 min. Afterwards, an equal volume of PCR product was blended with 1× loading buffer (containing SYB green) and used for detection by electrophoresis in 2% agARGsse gel. Samples with a bright main strip between 400 and 450 bp were chosen for subsequent experimentation. The selected PCR products were mixed to equidensity ratios and purified with Qiagen Gel Extraction Kit (Qiagen, Germany). Sequencing libraries were generated via a TruSeq® DNA PCR-Free Sample Preparation Kit (Illumina, California, United States). The quality of libraries was assessed using a Qubit@ 2.0 Fluorometer (Thermo Fisher Scientific, Massachusetts, United States) and an Agilent Bioanalyzer 2100 (Agilent, California, United States) system. The libraries were lastly subjected to Illumina NovaSeq (Illumina, California, United States) platform sequencing.

2.5 16S rRNA gene sequencing data analysis

Splitting each sample data from the paired end allows it to be read according to the unique barcode. After the barcode and primer sequences were truncated, the raw tags were generated by FLASH (ver.1.2.7) (Magoč, et al., 2011). Sequences from the raw data were analyzed and filtered by QIIME (ver.1.9.1) to obtain high-quality clean tags. Low-quality tags with quality value ≤ 19, homopolymer ≥ 3 bases, and consecutive high-quality bases < 75% were filtered out. Then, the quality-filtered tags were compared with the reference database (Silva Database) using the

191 UCHIME algorithm (Robert, et al., 2011) which detects and remove chimera sequences, finally
192 resulting in effective tags.

193 Sequences with ≥ 97% similarity were assigned to the same operational taxonomic units
194 (OTUs) by Uparse software (ver.7.0.1001) (Edgar, 2013). For each OTU-representative sequence,
195 the SILVA Database (Quast, et al., 2012) was used based on the MOTHUR algorithm to annotate
196 taxonomic information with an 80% confidence threshold. In preparation for later analysis, OTU
197 abundance information was normalized according to a sequence number standard corresponding to
198 the sample with the least sequence among the 9 samples. Furthermore, the differences in phyla and
199 genera between groups were compared using one-way analysis of variance (one-way ANOVA) and
200 Tukey's multiple comparisons. Subsequently, the alpha diversity and beta diversity were calculated
201 using QIIME software (ver. 1.7.0). The alpha diversity index included ACE, Chao1,
202 Observed-species, Shannon, Simpson, and Good's coverage. The beta diversity index was based on
203 the phylogenetic relationship between OTUs to calculate the Unifrac distance (weighted Unifrac),
204 and beta diversity results were shown through PCA. R software (ver.2.15.3) was used to analyze
205 PCA, UPGMA, and Venn diagrams based on OTUs. In order to further explore the differences in
206 community structure among the grouped samples, the LEfSe method was used to test the
207 significance of the differences in group composition and the community results of the grouped
208 samples to find different species (Segata, et al., 2011).

209 **2.6 Metagenome sequencing, data preprocessing and assembly**

210 Nine DNA samples from shrimp intestines (JI1, JI2 and JI3), water (JW1, JW2 and JW3), and
211 effluent (JT1, JT2 and JT3) were used for metagenome analysis by Novogene Biological
212 Information Technology Co. (Tianjin, China). The DNA quality and purity were assessed as

mentioned above. 1 μg of each sample was utilized as input material for the DNA sample preparations. Sequencing libraries were generated using NEBNext® Ultra™ DNA Library Prep Kit for Illumina (New England Biolabs, Massachusetts, United States) following the manufacturer's recommendations. Briefly, each DNA sample was randomly fragmented into 350 bp segments via sonication. PCR amplification was then performed after they were end-polished, poly A-tailed, and ligated with the full-length adaptor. The library preparations were sequenced on an Illumina HiSeq 2500 (Illumina, California, United States) platform and paired-end reads were generated.

The raw data obtained above was preprocessed using Readfq (V8) to acquire clean data for subsequent analysis. The specific processing steps are as follows: first, the reads which contained low quality bases (default quality threshold value ≤ 38) with a default length exceeding 40 bp were removed. Then, the reads in which the N base exceeded 10 bp were removed. Lastly, the reads with adapter contamination above a certain percentage were removed. After filtering, clean data were assembled into scaftigs by MEGAHIT software (ver. 1.0.4-beta) (Li, et al., 2015; Nielsen, et al., 2014). ORF prediction of scaftigs (≥ 500 bp) assembled from both single and mixed were performed using MetaGeneMark software (V2.10). Then, the results of the ORF prediction were made de-redundant via CD-HIT software (V4.5.8) to obtain a non-redundant initial gene catalogue (Fu, et al., 2012; Li, et al., 2006). Subsequently, the clean data of each sample was compared with the initial gene catalogue using Bowtie 2.2.4, and finally the unigenes were obtained for subsequent analysis.

2.7 Metagenomic analysis and resistance gene annotation

Unigenes were aligned with Bacteria, Fungi, Archaea, and Viruses sequences in the NR database (Version: 2018-01-02) from NCBI using DIAMOND software (V0.9.9), and the LCA

algorithm was applied to determine species annotation information for the sequence alignment results (Buchfink, et al., 2015). Relative abundance profiles at each taxonomic level were then displayed by Krona analysis (Ondov, et al., 2011). In the functional analysis, the unigenes were blasted with the KEGG database (Version: 2018-01-01) using DIAMOND software (V0.9.9) (Kanehisa, et al., 2014), and the best Blast Hit was selected out of each sequence alignment result for subsequent analysis (Li, et al., 2014). The relative abundance of each functional hierarchy was equal to the sum of relative abundance annotated to that functional level. In addition, heatmaps based on z-standardized values of normalized relative abundance were performed by R software (ver. 3.2.3).

Resistance Gene Identifier (RGI) software was used to align the unigenes to the CARD database (https://card.mcmaster.ca/) (Jia, et al., 2016; Martínez , et al., 2015) with parameter settings of blastp, evalue ≤ 1e-30. Based on the aligned results, the relative abundance of ARGs was counted. Based on the abundance of ARGs, the abundance bar charts, an abundance cluster heatmap, and the difference in the number of resistance genes between groups are displayed. Analyses of the abundance and distribution of resistance genes in each sample, the resistance genes' species attribution, and the resistance mechanism of the genes were also conducted.

2.8 Data availability and statistical analysis

The differences between groups were compared by one-way ANOVA and multiple comparisons of Tukey's HSD test using SPSS 17.0. A p value of < 0.05 was considered significant.

3. Results

3.1 Growth performance

Growth performance of *P. monodon* is presented in Table 1. After rearing for 105 days, the *P. monodon* samples had an average weight of 11.69 ± 0.92 g and an average length of 10.69 ± 0.66 cm. These data suggest that the growth of *P. monodon* occurred over three periods: between 0 and 15 days, rapid growth occurred with a SGR of 17.63%; between 30 and 60 days, steady growth occurred with a SGR of 5.20%–6.00%; and after day 75, slow growth occurred with a SGR of 0.75%–2.44%.

Table 1

Periodic growth performance of *P. monodon* cultured with "Fishery-PV Integration" engineering for 105 days.

Age (days)	Body length (cm)	Body weight (g)	Relative body length growth rate (%)	Relative body weight growth rate (%)	Specific growth rate (%)
0 d	0.74 ± 0.03	0.006 ± 0.001	—	—	—
15 d	2.65 ± 0.15	0.17 ± 0.02	257.30 ± 0.20	2559.13 ± 3.43	17.63 ± 0.06
30 d	3.69 ± 0.33	0.47 ± 0.15	38.94 ± 0.05	168.56 ± 0.53	5.20 ± 0.03
45 d	5.09 ± 0.33	1.29 ± 0.28	38.34 ± 0.04	181.95 ± 0.26	5.12 ± 0.02
60 d	7.17 ± 0.63	4.26 ± 1.23	40.73 ± 0.03	226.39 ± 0.24	6.00 ± 0.03
75 d	8.48 ± 0.67	6.64 ± 1.56	18.34 ± 0.03	58.08 ± 0.12	2.12 ± 0.01
90 d	9.80 ± 0.18	10.30 ± 0.59	12.33 ± 0.04	61.41 ± 0.27	2.44 ± 0.01
105 d	10.69 ± 0.66	11.69 ± 0.92	9.04 ± 0.05	13.40 ± 0.03	0.75 ± 0.003

Data represent growth performance means ± SD from three repetitions.

3.2 Analysis of the changes in content of nitrogen in the aquaculture water of "Fishery-PV Integration" ponds

The variation in levels of ammonia nitrogen, nitrite, and nitrate in the aquaculture water of the "Fishery-PV Integration" ponds is shown in Fig. 2a. Ammonia nitrogen concentration was maintained at a low level during the rearing period and reached its highest value (1.57 mg/L) when the shrimp were 75 days old. Nitrite levels showed an increasing trend until the shrimp were 85

days of age, where it reached a maximum value of 4.30 mg/L. Nitrate levels peaked when the shrimp were 75 days old at 13.41 mg/L. Throughout the culture trial, the pH and temperature of the seawater remained at ~ 7.86 and ~ 29.93 ℃.

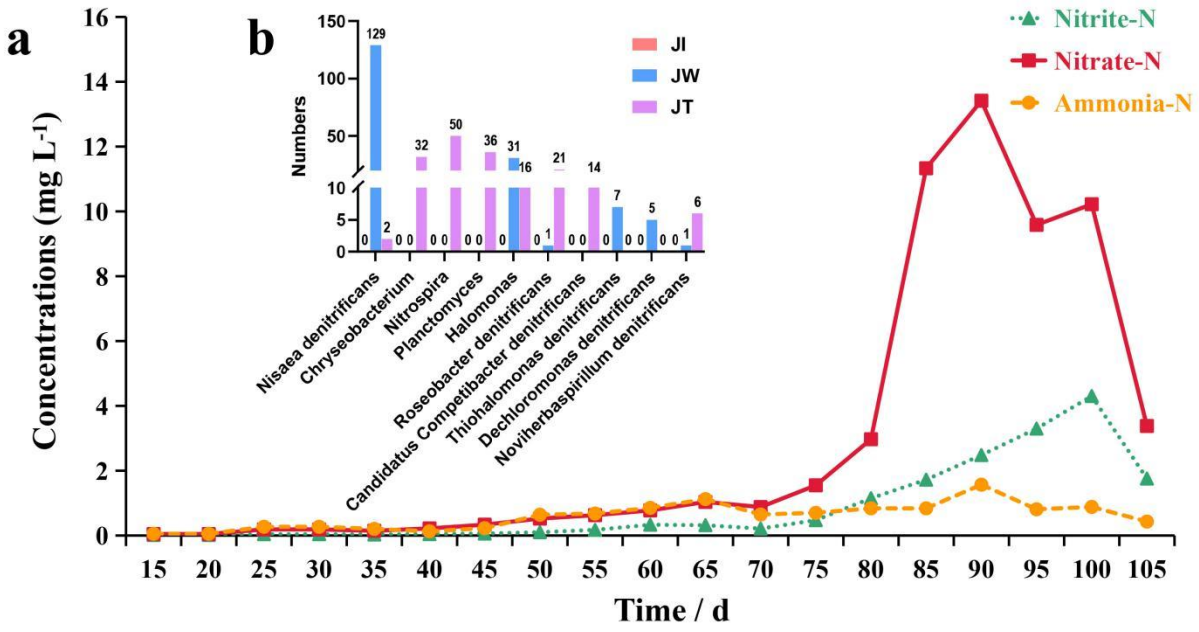

Fig. 2. (a) Concentration of ammonia nitrogen (Ammonia-N), nitrite (Nitrite-N), and nitrate (Nitrate-N) over time in the "Fishery-PV Integration" ponds. (b) Bar plots shows the distribution of 10 common denitrificans in the pond. The y-axis shows the number of genes annotated to the bacteria; the x-axis shows the name of the denitrificans.

3.3 Amplicon sequencing results

As shown in Table 2, 77,786-100,016 raw tags, 76,688-98,141 clean tags, 55,500–68,243 effective tags, and 53,443-66,802 taxon tags were obtained from nine samples. In addition, the average effective tags length was 413 to 428 nt. After quality filtering and trimming, 898 to 2,044 operational taxonomic units (OTUs) were detected using 97% identity as the cutoff in the samples. Good's coverage estimations indicated that 99.2%-99.6% of the species were identified in all nine

283 samples. Alpha diversity analysis showed that the Shannon index ranged from 1.016 to 6.765, while
284 the Simpson index ranged from 0.156 to 0.947, the Chao1 index from 873.392 to 2045.065, and the
285 ACE index from 925.341 to 2102.897. Community richness indices (ACE and Chao1) and
286 community diversity indices (Simpson and Shannon) showed that the richness and diversity of the
287 water and effluent were significantly higher than that of the shrimp intestine ($P < 0.01$) (Table 3).

Table 2

16S rRNA gene sequencing results of 9 samples of shrimp intestine (JI), water (JW), and effluent (JT).

Sample name	Number of raw tags	Number of clean tags	Number of effective tags	Average length of effective tags	Number of taxon tags	Number of unique tags	Number of OTUs
JI1	82,445	79,762	65,703	428	64,525	1,077	898
JI2	100,016	98,141	66,129	424	60,346	5,742	1,077
JI3	85,469	83,872	67,671	428	66,802	848	934
JW1	79,877	78,459	55,500	413	53,443	2,014	1,854
JW2	93,395	92,258	61,212	414	58,620	2,583	1,942
JW3	92,987	91,625	63,645	415	60,779	2,840	1,931
JT1	93,624	92,393	68,243	414	65,281	2,925	2,044
JT2	88,182	87,085	62,222	414	59,263	2,955	1,973
JT3	77,786	76,688	57,879	414	55,530	2,342	1,966

Table 3

Alpha diversity indices of shrimp intestine, water, and effluent.

Sample name	Observed species	Shannon	Simpson	Chao1	ACE	Good's coverage
JI1	740	1.016	0.156	873.392	925.341	0.995
JI2	919	3.057	0.578	1053.759	1073.618	0.995
JI3	777	1.098	0.162	890.569	948.423	0.996
JW1	1663	6.132	0.912	1828.509	1884.211	0.993

JW2	1740	6.595	0.936	1887.736	1937.930	0.993
JW3	1736	6.765	0.947	1943.000	1976.384	0.993
JT1	1838	6.505	0.933	2045.065	2102.897	0.992
JT2	1764	6.545	0.94	1972.348	1989.933	0.993
JT3	1774	6.757	0.945	1955.654	1983.287	0.993
Mean ± S.D.						
JI	812 ± 94.493[b]	1.724 ± 1.155[b]	0.298 ± 0.242[b]	939.240 ± 99.548[b]	982.461 ± 79.784[b]	0.995 ± 0.001[b]
JW	1713 ± 43.347[a]	6.497 ± 0.328[a]	0.932 ± 0.179[a]	1886.415 ± 57.257[a]	1932.842 ± 46.297[a]	0.993 ± 0.000[a]
JT	1792 ± 40.150[a]	6.602 ± 0.135[a]	0.939 ± 0.006[a]	1991.022 ± 47.541[a]	2025.372 ± 67.221[a]	0.993 ± 0.001[a]

Values are presented as mean ± S.D. (n= 3). Dissimilar letters show extremely significant difference ($p < 0.01$).

3.4 Comparison analysis of microbial composition of shrimp intestines, water, and effluent in "Fishery-PV Integration" ponds

The 16S rRNA genes from the shrimp intestines, water, and effluent were sequenced to study the bacterial community structure of the "Fishery-PV Integration" ponds. According to the abundance of taxa, OTUs were identified as being from 61 phyla. Within effluent (JT) and water (JW) samples, the dominant phyla (relative abundance > 2%) were the same. Proteobacteria (48.90%, 51.01%) was the most abundant phyla in the effluent and water samples, followed by Actinobacteriota (9.30%, 9.14%), Bacteroidota (3.88%, 4.32%), and Verrucomicrobiota (2.73%, 3.22%), in total accounting for 64.81% and 67.69% of all sequences, respectively. The other divisions consistently found in the two groups were Firmicutes and Acidobacteriota (Fig. 3a). In shrimp intestinal microbiota (JI), Proteobacteria was the most abundant phyla, accounting for over 92% of all sequences in intestinal samples. In the intestinal samples, most OTUs were mapped to Proteobacteria (Fig. 3b), and there was a significant difference between the other two groups ($p < 0.05$). In addition, the abundance of Actinobacteriota, Verrucomicrobiota, and Bacteroidota in water and effluent group was upregulated significantly. In the water group, the relative abundance of

Firmicutes was significantly increased compared with the other two groups. Interestingly, the microbiota in the water samples closely matched the effluent samples (Fig. 3c).

When the OTUs were considered at the genus level, a total of 673 taxa were identified in all samples. The top 6 most common genera were *Ralstonia*, *Candidatus Aquiluna*, *Vibrio*, *Roseivivax*, *Terrimicrobium,* and *Marivita* (Fig. 4a). Compared with the water and effluent samples, the relative abundance of *Ralstonia* in intestinal samples was significantly increased ($p < 0.05$) (Fig. 4b). In contrast, the relative abundance of *Candidatus Aquiluna*, *Marivita* and *Roseivivax* in the water and effluent group was higher than intestinal group. The abundance of *Vibrio* in the intestinal samples was higher, but still at a relatively low level overall, and there was no significant difference among the groups ($p > 0.05$) (Fig. 4c). We also screened 10 common denitrificans for characterization at the species level, including *Nisaea denitrificans*, *Chryseobacterium*, *Nitrospira*, *Planctomyces*, *Halomonas*, *Roseobacter denitrificans*, *Candidatus Competibacter denitrificans*, *Thiohalomonas denitrificans*, *Dechloromonas denitrificans*, *Noviherbaspirillum denitrificans* (Fig. 2b).

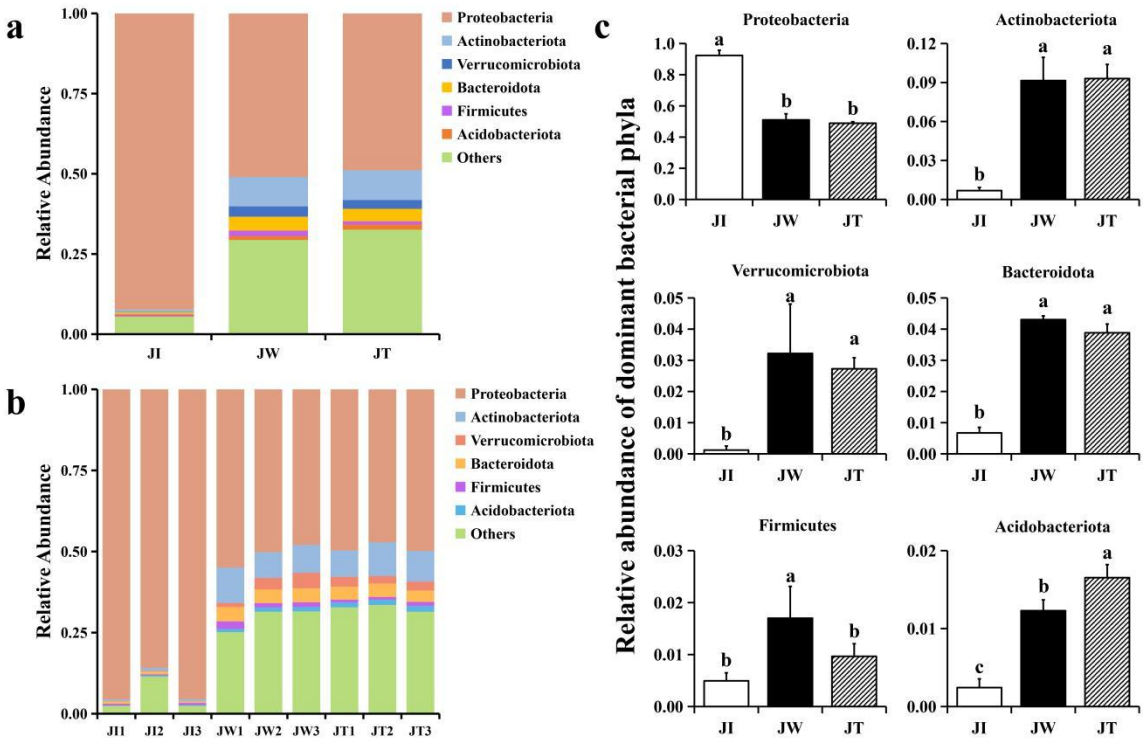

Fig. 3. Structure and composition of the intestinal bacterial communities among shrimp intestines (JI), water (JW), and effluent (JT) in "Fishery-PV Integration" ponds at the phylum level of taxonomy. (a) Relative abundance of phyla across the three groups, (b) the phyla appearing in each sample, and (c) changes in the abundance of dominant bacterial phyla. Data are presented as mean ±SD. Dissimilar letters show significant differences and the statistically significant differences between the two groups were calculated by Student's t-test ($P < 0.05$).

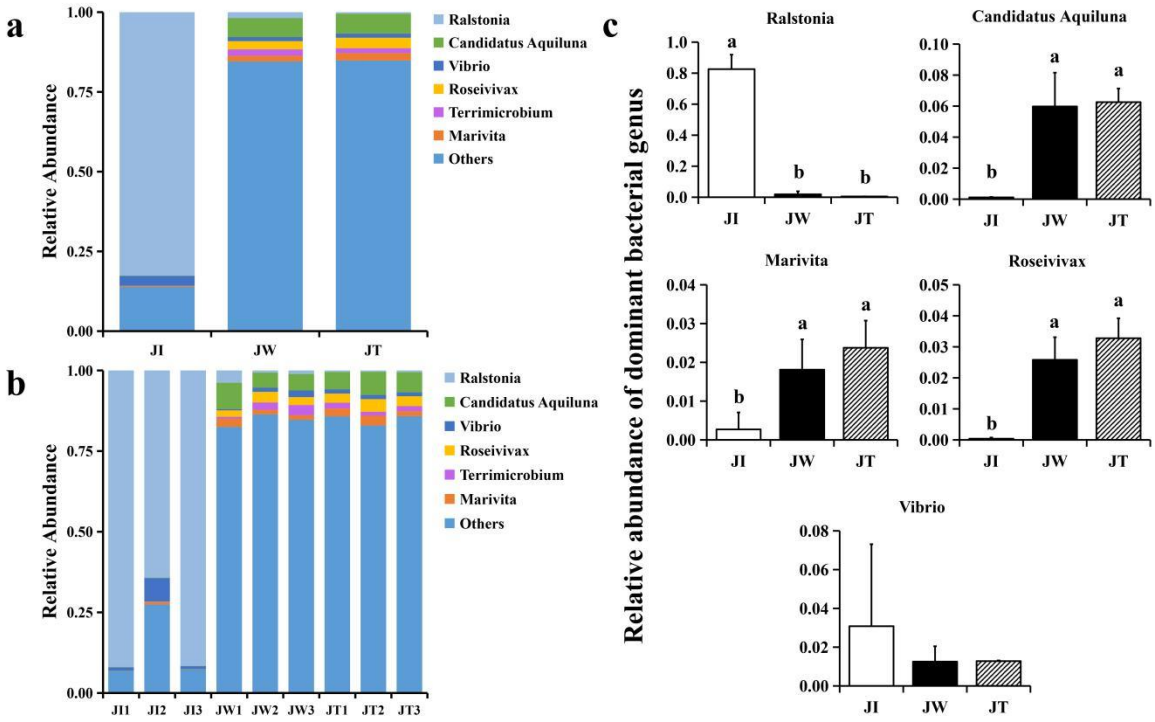

Fig. 4. Structure and composition of the intestinal bacterial communities among shrimp intestines (JI), water (JW), and effluent (JT) in "Fishery-PV Integration" ponds by genus. (a) Relative abundance of phyla across the three groups, (b) the phyla appearing in each sample, and (c) the changes in abundance of dominant bacterial genera. Data are presented as mean ± S.D. Dissimilar letters show significant differences and the statistically significant differences between the two groups were calculated by Student's t-test ($P < 0.05$).

3.5 The relationships among microbial communities found in shrimp intestines, water. and

effluent in "Fishery-PV Integration" ponds

The Venn figure demonstrates that the sequences found in shrimp intestinal, water, and effluent samples were clustered into 1631, 2821, and 2817 OTUs, respectively (Fig. 5a). 928 OTUs were shared between JI, JW, and JT, accounting for 22.82% of the identified OTUs. Additionally, *Proteobacteria* was the most abundant phylum among the shared OTUs, accounting for 31.25% (290 OTUs). It is noteworthy that the percent of OTUs shared by JI and JW, JI and JT, and JW and JT were 28.37%, 25.30%, and 47.87%, respectively, indicating that JW and JT shared more identical OTUs. A PCA plot was used to reveal the compositions of the microbial communities found in shrimp intestines, water, and effluent in the "Fishery-PV Integration" ponds. As shown in Fig. 5b, the first two components explain a total of 36.84% of the variation (PC1, 22.97%; PC2, 13.87%). This figure also illustrates that JW and JT samples were closely clustered, while JI samples tended to cluster separately. UPGMA cluster analysis revealed that JW and JT were clustered together (Fig. 5c). Simultaneously, weighted UniFrac analysis showed that the abundance of groups found in the JW and JT samples was lower than that of the JI samples. The flora found in the JW samples was most like that of the JT group (Fig. 5d). Overall, this data indicates that the compositions of microbial communities was most similar between the JW and JT groups in the "Fishery-PV Integration" ponds.

LEfSe analysis was used to reveal specific taxa associated with each sample. As shown in Fig. 6, LEfSe analysis was conducted between JI, JW, and JT. The bar chart indicates that 11 specific taxa were identified with a LDA score of >4 (Fig. 6a). JI had more specific taxa than did JT and JW. The relevant taxa in JI, JT, and JW were g_Ralstonia, s_Ralstonia_pickettii, f_Burkholderiaceae, o_Burkholderiales and c_Gammaproteobacteria; p_unidentified_Bacteria, c_Bacteroidia,

o_Chitinophagales, and f_Saprospiraceae; c_Bacteroidia and p_Bacteroidota, respectively. Evolutionary branch diagrams of LEfSe analysis based on classification information are given in Fig. 6b, which shows the different information of all bacteria at the phylum, class, order, family, and genus levels.

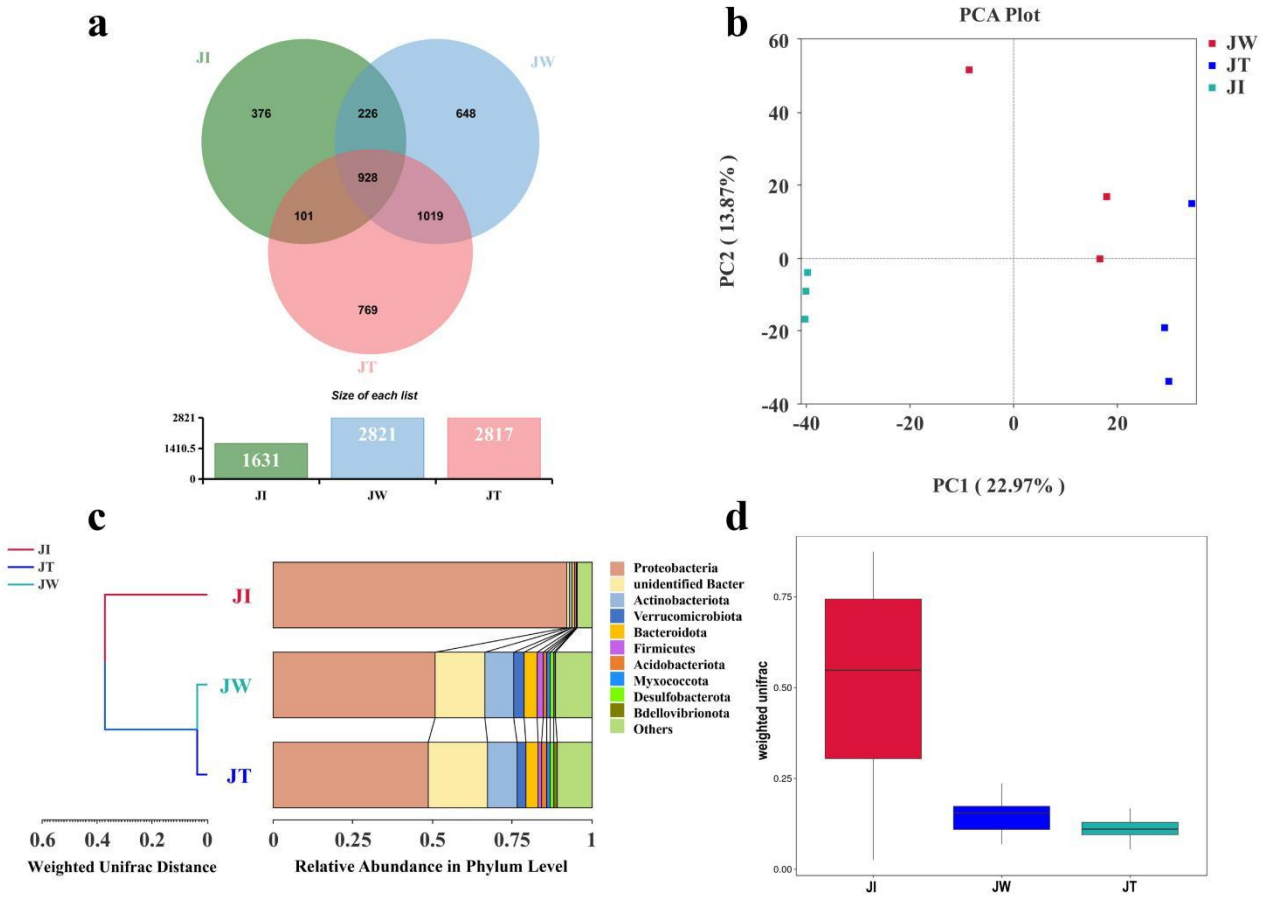

Fig. 5. Associations between microbial communities of shrimp intestines, water, and effluent in "Fishery-PV Integration" ponds. (a) Venn diagram of unique and shared bacterial OTUs from intestinal contents (JI), water (JW), and effluent (JT). (b) PCA (Principal Components Analysis) distribution plot; samples from the same group are clustered closer. (c) UPGMA clustering tree based on the Weighted UniFrac distance at the phylum level. The length of the branches represents the distance between the samples. If the composition of the microbial

communities in the samples is similar, they will be clustered together in the clustering tree. (d) Weighted UniFrac analysis of intestinal contents (JI), water (JW), and effluent (JT).

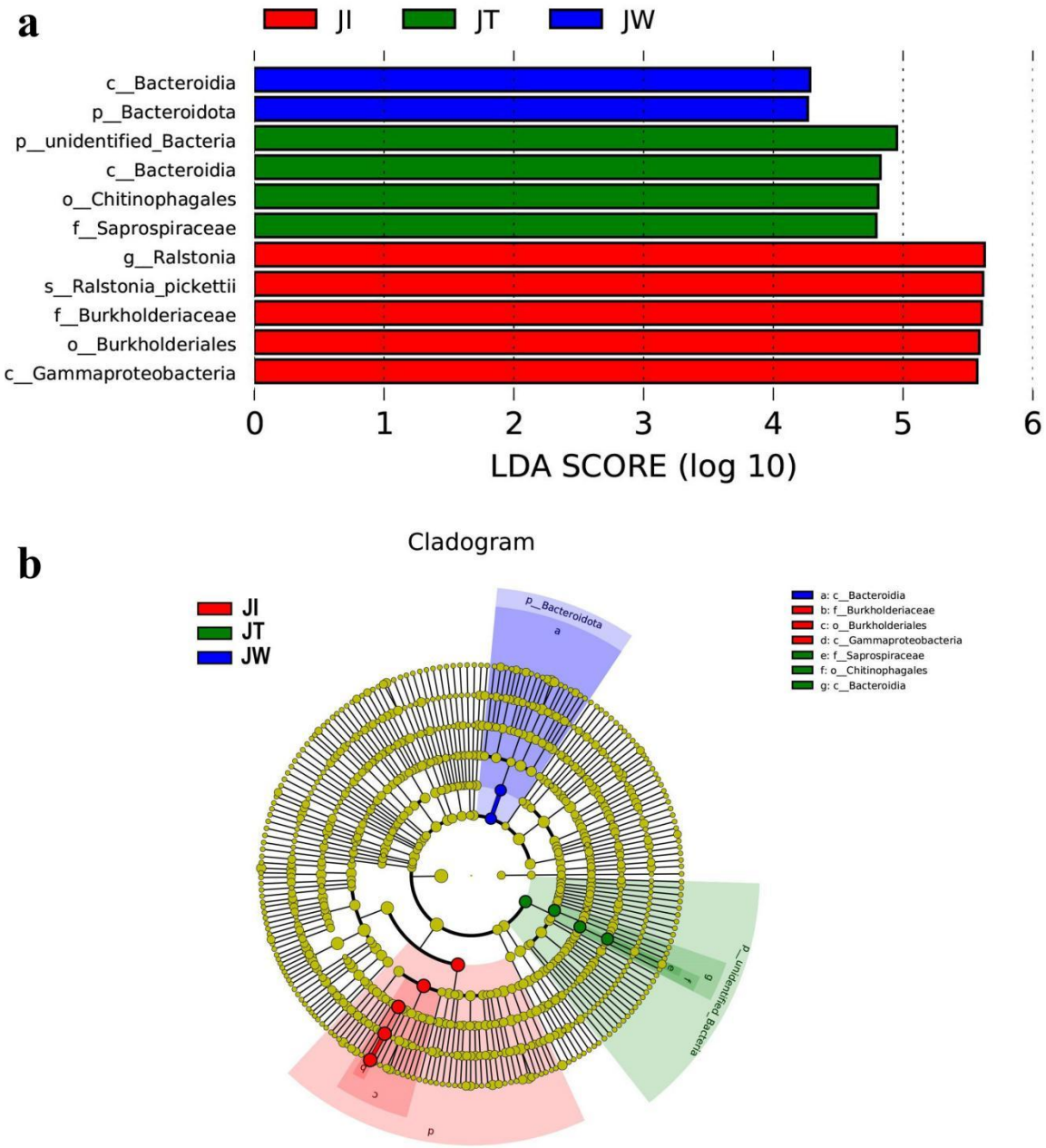

Fig. 6. LEfSe analysis of JI, JW, and JT. (a) Only taxa with LDA value (influence value of linear discriminant analysis) higher than four were shown. (b) Evolutionary branch graph of differential bacterial communities or species.

3.6 Metagenome sequencing results

In this study, the microbial DNA samples from shrimp intestines, water, and effluent were sequenced using the Illumina HiSeq platform. The data showed that a total of 6323.49–6642.93 M bp of raw data and 6315.43–6534.97 M bp of clean data were obtained from samples JI, JW, and JT. After single-sample and hybrid assembly, 1,844–87,963 scaftigs were obtained with an average N50 of 1371 bp. 2,230–155,869 ORFs (open reading frames) were generated and annotated by MetaGeneMark software (Version 2.10). Taxonomic classification according to metagenome showed that most reads in the JW and JT groups were assigned to Bacteria (57.00%–61.67%), whereas the proportion of bacteria in the JI group was only 14%. The relative abundance of Bacteria, Archaea, Eukaryota, and Viruses was 14.00–61.77%, 0.01–0.30%, 0.13–0.33%, and 3.67–5.63%, respectively (Table 3). Fig. 7 shows the top 10 dominant bacterial phyla and genera based on the metagenome sequencing profiles. It was observed that *Proteobacteria* was the most abundant phyla found in all samples (Fig. 7a). At the genus level, the abundance of *Vibrio* in JI was higher than that of JW and JT (Fig. 7b). These results are consistent with the amplicon sequencing results.

Table 4

Statistics of metagenome sequencing data from JI, JW, and JT in “Fishery-PV Integration” ponds.

	JI	JW	JT
Raw data (M bp)	6642.93	6367.31	6323.49
Clean data (M bp)	6534.97	6359.22	6315.43
No. of scaftigs	1,844	87,963	76,313
Total length of scaftigs	5,026,119	370,738,681	294,271,095
N50 length (bp)	860	1785.67	1470
Predicted ORFs	2,230	184,268	155,869
Unigenes	5,409	194,233	213,784
Unigenes annotated on KEGG	3,689(68.20%)	85,904(44.23%)	83,608(39.11%)
Unigenes annotated on EggNOG	3,586(66.30%)	83,872(43.18%)	78,195(36.58%)
K__Bacteria	14.00%	57.00%	61.67%
K__Archaea	0.01%	0.30%	0.27%
K__Eukaryota	0.17%	0.33%	0.13%
K__Viruses	4.00%	5.33%	3.67%

Unclassified	81.83%	37.03%	34.27%

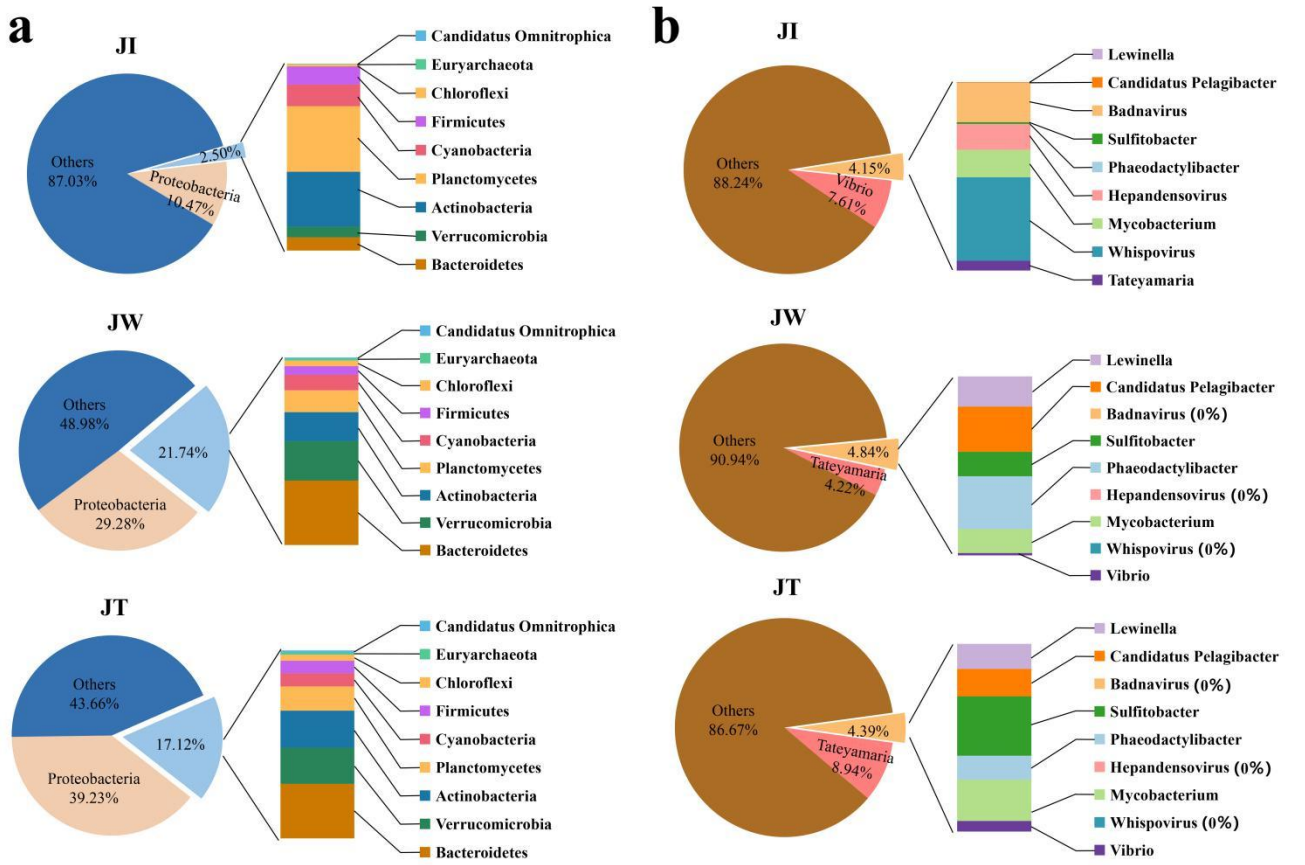

Fig. 7. Relative abundances of top 10 dominant bacterial phyla (a) and genus (b) among water (JW), effluent (JT), and shrimp intestines (JI) based on the metagenome sequencing profiles.

3.7 Functional studies of microbial groups in "Fishery-PV Integration" ponds

Fig. 8a indicates that water (JW) and effluent (JT) microbiota had more functional genes than shrimp intestine (JI) samples, suggesting that shrimp intestinal microbiota have functional pathways distinct from those of the water and effluent microbial communities. In KEGG level 1, a high proportion of the gene annotations in shrimp intestines, water, and effluent were mainly associated with "Metabolism," "Human Diseases," "Genetic Information Processing," "Environment Information Processing," and "Cellular Processes." Within KEGG level 2, carbohydrate metabolism, amino acid metabolism, energy metabolism, and metabolism of cofactors and vitamins were the

most predominant metabolism types in the metabolism category. The dominant pathways in "Environmental Information Processing" were membrane transport and signal transduction. In the "Genetic Information Processing" category, the most abundant pathways were translation; replication, repair, and folding; and sorting and degradation. The "Cellular Processes" category was dominated by cellular community, cell growth and death, and cell motility pathways. Additionally, 35 of the most abundant pathways at the third level of KEGG are displayed in Fig. 8b, among which the most abundant pathways were ABC transporters (ko02010), purine metabolism (ko00230), pyrimidine metabolism (ko00240), quorum sensing (ko02024), two-component system (ko02020), and oxidative phosphorylation (ko00190). Moreover, heatmaps of the top 35 most abundant KEGG level 2 (Fig. 9a) and level 3 pathways (Fig. 9b) are presented. As Fig. 9b suggested, two (ko05034, ko05322), four (ko00670, ko00240, ko00790, ko00970), and eighteen (ko02010, ko02020, ko03070, ko00680, ko00360, ko00630, ko00260, ko02024, ko00280, ko00860, ko00330, ko00650, ko00720, ko00010, ko00051, ko00640, ko00620, ko00030) pathways were notably enriched in JI, JW, and JT, respectively.

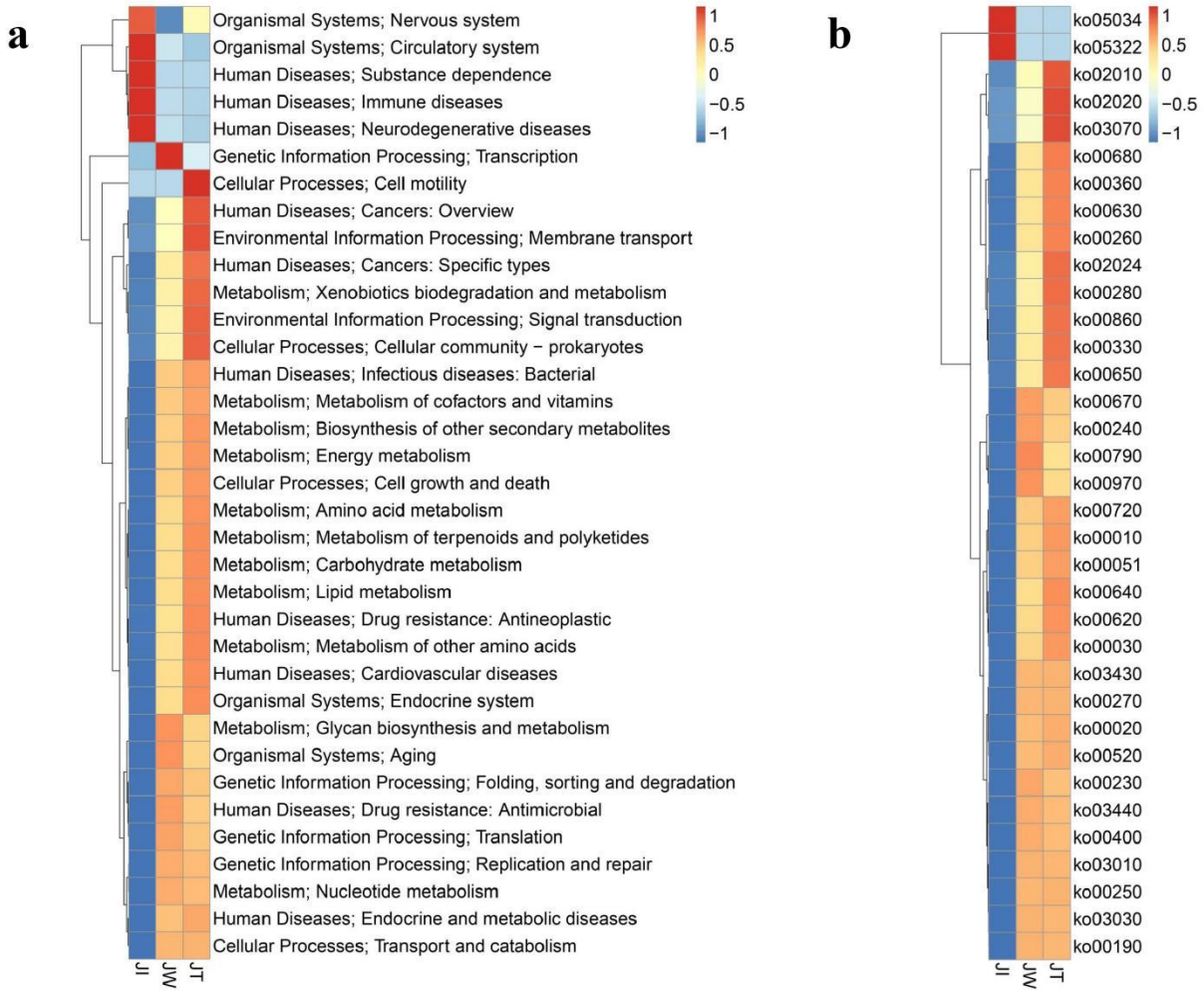

410

411 **Fig. 9.** Heatmaps of top 35 abundant KEGG level 2 (a) and level 3 (b) functional categories based

412 on z-standardized values of normalized relative abundance between JI, JW, and JT.

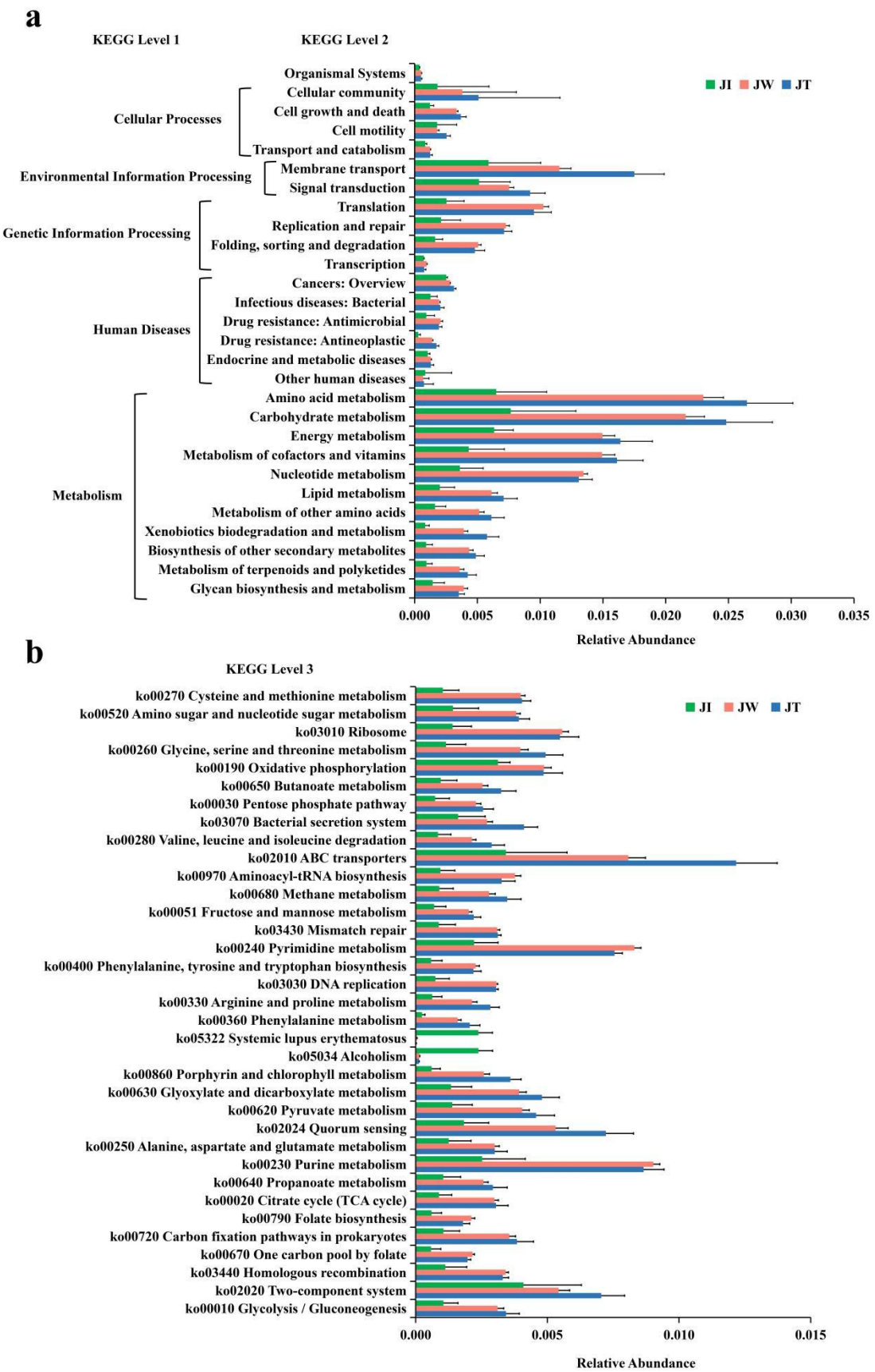

Fig. 8. Normalized relative abundance of Unigenes of KEGG level 2 (a) and top 35 abundant KEGG level 3 (b) functional categories in JI, JW, and JT. Data are presented as mean ± S.D.

3.8 Resistance gene annotation of microbiota in "Fishery-PV Integration" ponds

The resistance gene annotation results showed that 123 kinds of ARGs were identified in the shrimp gut, pond water, and effluent samples. The relative abundance of ARGs in all samples are shown in Fig. 10a. In general, the relative abundance of the total ARGs found in JI, JW, and JT were 0.49-2.22 × 10^{-4} ppm, 2.59-2.76 × 10^{-4} ppm, and 3.71-4.27 × 10^{-4} ppm, respectively. Notably, ARGs were significantly more abundant in water and effluent samples than in intestinal samples. As showcased in Fig. 10b, the ARGs of the intestinal group were dominated by *tetH* (10.19-26.56%), *QnrVC6* (10.03-23.07%), and *tetX* (0.98-25.62%). Conversely, in the water and effluent groups, the ARGs with the highest relative abundance were *MexL* and *adeF,* ranging from 9.78% to 14.81%, respectively, in the water group, and 11.84% to 15.29%, respectively, in the effluent group. Fig. 10c shows the association between the resistance mechanism and bacteria in all samples. Antibiotic inactivation and efflux pump were the predominant resistance mechanisms in all samples, with 57 and 48 resistance genes, respectively. Additionally, among the 45 resistance genes successfully annotated to the bacteria, 26 resistance genes were annotated to Proteobacteria. The two-circle diagram shows the relationship between resistance genes and species attribution in the JI, JW, and JT groups (Fig. 10d). In JI, bacterial ARGs were mainly derived from Proteobacteria (32%), Planctomycetes (5%), and Actinobateria (6%), while in JW, bacterial ARGs were mainly found to be from Proteobacteria (23%) and Bacteroidetes (8%). Similarly, bacterial ARGs in JT were established to be mainly from Proteobacteria (23%) and Bacteroidetes (7%).

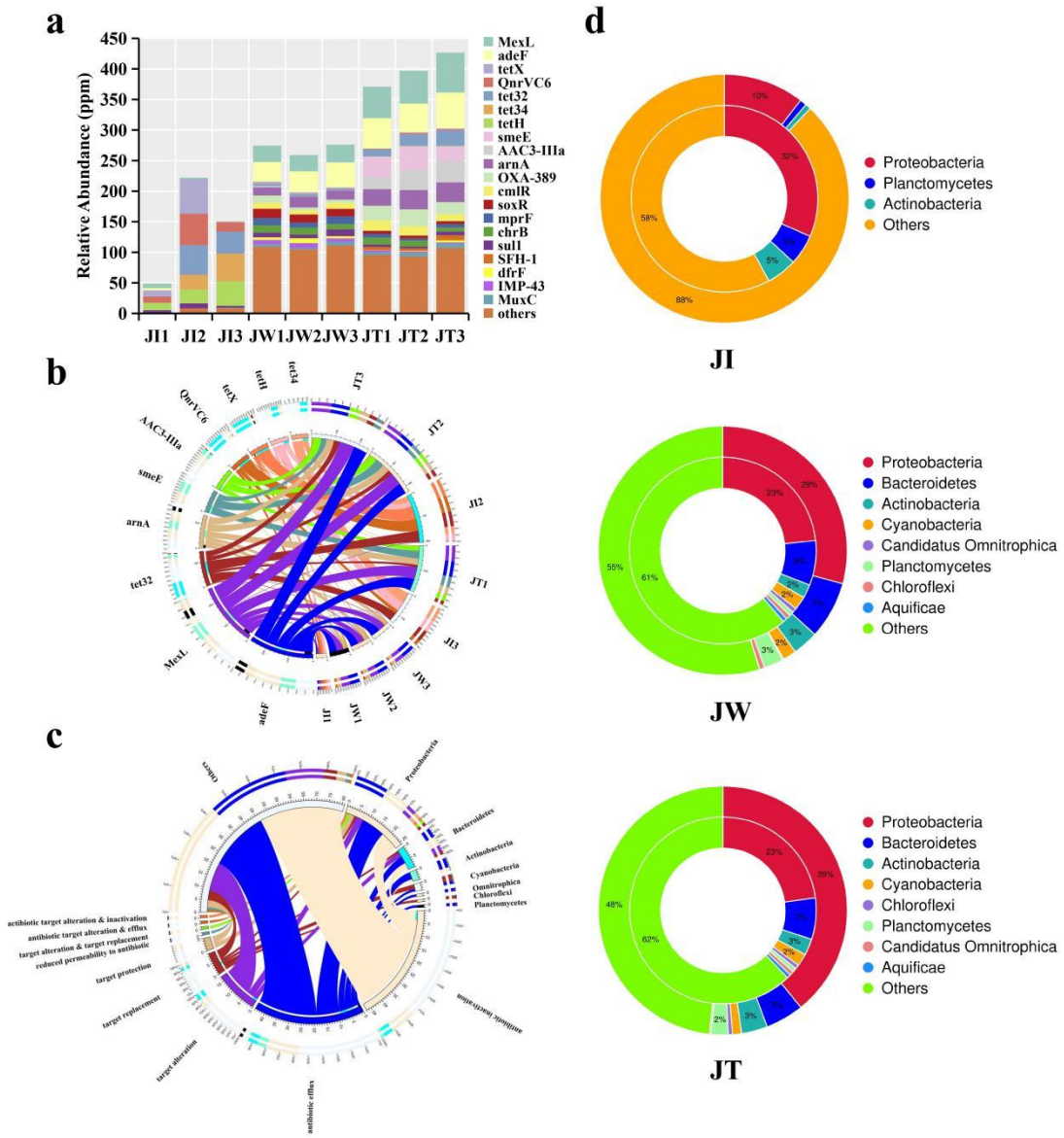

Fig. 10. Results of resistance gene annotation in intestinal, water, and effluent samples in "Fishery-PV Integration" ponds. (a) Indicates the relative abundance of all the genes in each sample of ARGs (in ppm, the result of magnifying the original relative abundance data 10^6 times). (b) The 10 most abundant ARGs were plotted to a circle diagram. The circle diagram was divided into two parts: ARGs information on the left, and sample information on the right. Different colors of the inner ring represent different samples and ARGs, and their scale represents their relative abundance in ppm. (c) The circle diagram consists of two parts. On the right side is the species information at the phylum level, and the left side shows resistance mechanism information. The

different colors in the inner circle indicate the resistance mechanisms of different species and resistances, and the scale represents the number of genes. The left side shows the sum of the number of resistance genes in the species that contain this type of resistance mechanism, and the right side shows the sum of the number of resistance genes contained in different resistance mechanisms. (d) Species identification analysis of ARGs in JI, JW, and JT. The inner circle represents the species distribution of ARGs, and the outer circle represents the species distribution of all genes in the group.

4. Discussion

Presently, the traditional aquaculture model is overly simplified, with an environment that is susceptible to outside influence (Haro-Moreno, et al., 2020). The construction of a safe, stable, and economical aquaculture model is of immediate importance to the sustainable development of the aquaculture industry. In recent years, the “Fishery-PV Integration” culture mode has received widespread attention. This mode integrates PV power generation, which not only effectively improves land utilization rates, but is also conducive to the development and utilization of new energy, thus being beneficial to both agriculture and industry (Pringle, et al., 2017). However, its effect on the ecological environment of aquaculture and the growth rate of shrimp remains unclear. Therefore, in this study, a metagenomics approach combined with 16S rRNA gene sequencing were used to investigate the structure and function of bacterial communities and the diversity of ARGs in three *P. monodon* “Fishery-PV Integration” ponds in Guangxi Province, China. The water quality index and the growth rate of *P. monodon* were measured and recorded at regular intervals. This study comprehensively analyzed the characteristics of microflora in the “Fishery-PV Integration” ecosystem.

Our results indicated that Proteobacteria, Actinobacteriota, and Bacteroidota were the predominant phylum in water, effluent, and shrimp intestines, consistent with the levels found in the freshwater and marine cultured environment of *P. vannamei* (Fan, et al., 2019), freshwater crab aquaculture environments (Fang, et al., 2019), and *P. monodon* biofloc-based aquaculture environments (Chen, et al., 2022). It is important to understand the bacterial groups with competitive advantages in shrimp intestines and the surrounding environments of cultured animals for the screening of probiotics in aquaculture. In the present study, metagenomics and 16S rRNA gene sequencing showed that Proteobacteria was the most dominant bacteria among the shrimp intestines, water, and effluent, and the abundance of Proteobacteria in intestinal samples was significantly higher than that of the surrounding water and effluent in shrimp ponds ($p < 0.05$). Some studies have revealed that the colonization potential is another important criterion to characterize probiotics (Gatesoupe, 1999), which seems to suggests that more attention should be paid to screening potential probiotics from Proteobacteria (He, et al., 2020). Furthermore, we observed that 31.25% shared OTUs were annotated to Proteobacteria, indicating that Proteobacteria played a significant role in microbial connections between shrimp intestines, water, and effluent. In addition, it was noted that the abundance of Verrucomicrobiota and Acidobacteriota in the water and effluent were high. Verrucomicrobiota can hinder algae bloom onset by consuming fucose (Orellana, et al., 2021), while Acidobacteriota promotes the material cycle (Flieder, et al., 2021). These two kinds of bacteria may play a vital role in maintaining the homeostasis of the “Fishery-PV Integration” culture environment. It is worth noting that at the genus level, we found that *Vibrio* was relatively less abundant. Previous studies indicated that *Vibrio* was one of the most abundant genera found in the shrimp gut (Fan, et al., 2019; Huang, et al., 2018b). The overabundance of *Vibrio* could

489 change the health status of shrimp and increase the risk of disease outbreaks (Xiong, et al., 2017).
490 However, the sampled shrimp were healthy, and no disease occurred during the experiment period.
491 Thus, we can speculate that the intestinal microbial flora of shrimp in this culture mode were stable,
492 which is beneficial to the healthy growth of shrimp. Water quality data indicated that levels of
493 ammonia nitrogen, nitrite, and nitrate showed a consistent trend during the breeding period, with
494 maximum values reached between 65 and 85 d, which may be related to the rapid growth of shrimp
495 and increased feeding (Liu, et al., 2017). Additionally, a large number of nitrifying and denitrifying
496 bacteria were identified in the water and effluent, including *Nisaea denitrificans* (Urios, et al., 2008),
497 *Halomonas* (Wang, et al., 2021), *Nitrospira* (Zhang, et al., 2014), *Dechloromonas denitrificans* and
498 *Planctomyces* (Feng, et al., 2019), etc., which all play a role in the nitrogen fixation process.
499 Therefore, the enrichment of nitrogen-fixing bacteria may be the one of the reasons for the rapid
500 decline of the average contents of ammonia, nitrite, and nitrate in the later cultured period.
501 Comparing with water and effluent, *Ralstonia* in shrimp intestines increased significantly. Curiously,
502 *Ralstonia* has been studied more in plants, but less in aquaculture (Ju, et al., 2021). In this study,
503 given that *Ralstonia* has the highest abundance in the gut, we believe that it is necessary to conduct
504 in-depth research on the physiological health of *Ralstonia* in shrimp. Additionally, *Candidatus*
505 *aquiluna*, *Roseivivax*, *Terrimicrobium,* and *Marivita* were significantly more abundant in water and
506 effluent than in the shrimp gut, but there was no significant difference between the water and
507 effluent groups. Similarly, we found that water and effluent richness (ACE and Chao1) and diversity
508 (Simpson and Shannon) were significantly higher than the richness and diversity of shrimp
509 intestines through the analysis of alpha diversity and beta diversity. There was no significant
510 difference in the diversity and richness of the water and effluent, indicating that the microbial

511 composition of the water and effluent groups were similar. It is possible that feed residue and
512 shrimp excrement provided a suitable nutritional growth environment for microflora in the water
513 and effluent (Cornejo-Granados, et al., 2017), which led to higher microbial richness and diversity
514 in the water and effluent compared to the intestines. It is worth noting that the diversity index of
515 intestinal microflora was low. There are studies indicating that the reduction of intestinal microbial
516 diversity (alpha diversity and beta diversity) may lead to the decrease of functional microflora and
517 weaken the host's ability to resist the invasion of pathogens (Fändriks, 2017). Therefore, an
518 appropriate amount of probiotics should be added to the “Fishery-PV Integration” pond in time to
519 reduce the risk of disease outbreaks.

520 KEGG level 1 and level 2 annotation results showed that metabolism—particularly amino acid
521 metabolism, carbohydrate metabolism, and energy metabolism—was dominant in the functional
522 categories of microorganisms, followed by environmental and genetic information processing,
523 consistent with many previous studies (LeBlanc, et al., 2017; Schweinitzer, et al., 2010). In the
524 intestinal microflora, the abundance of functional pathways related to carbohydrate and energy
525 metabolism was high, similar to the results of previous studies in shrimp, pandas, and turbot (Xing,
526 et al., 2013; Zhu, et al., 2011). One probable reason is that *P. monodon* digest carbohydrates for
527 energy through the intestinal microflora. In addition, amino acid metabolism pathways were more
528 abundant in water and effluent samples than in intestines, likely because unutilized nutrients or
529 feeds exist in water and effluent, providing a suitable living environment for microbiota that can
530 make use of amino acids. In-depth analysis based on KEGG level 3 classification reveals that ABC
531 transporters (ko02010) were more abundant in water and effluent. It has been reported that ABC
532 transporters are large membrane-bound proteins; their functions has been identified to mediate the

transport of various substrates including amino acids, lipids, sugars, and proteins (Chen, et al., 2001). This further indicates that there is a large amount of energy production and biosynthesis in the microflora of water and effluent in the "Fishery-PV Integration" ponds. Furthermore, the researchers believe that the ABC transporters play a vital role in the mechanism of protection against environmental toxins in aquatic invertebrate (Zhou, et al., 2009), suggesting that ABC transporters might be an important pathway for cell detoxification in shrimp to deal with high concentrations of ammonia nitrogen and nitrite. Quorum sensing (QS, ko02024) was underrepresented in JI, but overrepresented in JW and JT microbiotas. As a ubiquitous communication system among bacteria, QS not only mediates the formation of bacterial biofilm, but also regulate the secretion of virulence factors (Dickschat, 2010). In addition, QS is also an important mechanism for regulating the physiological and metabolic activities of microbial communities (He, et al., 2020). Thus, the presence of QS may significant implications for the health of the "Fishery-PV Integration" pond ecosystem. In conclusion, microorganisms in the "Fishery-PV Integration" culture mode not only promote intestinal digestion and absorption of shrimp, but also help to keep the water quality stable.

In recent years, environmental pollution caused by ARGs has become an increasing public health concern (Martínez, et al., 2015). As a new aquaculture model, it is necessary to evaluate the security and ecological impact of the "Fishery-PV Integration" pond by analyzing its ARGs. Rapidly developed metagenomics can be used to assess and track sources of environmental ARGs pollution (Li, et al., 2020a). In this research, the relative abundance of total ARGs in the "Fishery-PV Integration" pond was about 0.49-4.27 × 10^{-4} ppm, which was lower than the relative abundance of ARGs in *P. monodon* biofloc culture (2.46-5.82×10^{-4} ppm) (Chen , et al., 2022) and

555 coastal industrial mariculture systems (0.27-4.55×10^{-4} ppm) (Wang, et al., 2018). Furthermore, a
556 total of 123 ARGs were identified in the "Fishery-PV Integration" ponds, which was also
557 significantly lower than the number found in biofloc culture ponds (483 ARGs) (Chen, et al., 2022)
558 and freshwater shrimp culture ponds (229 ARGs) (Zhao, et al., 2018), indicating that "Fishery-PV
559 Integration" culture ponds are less easily enriched by ARGs than are other aquaculture ponds and
560 thus are safer in terms of public health. Recent studies have found that ARGs in aquaculture will
561 eventually enter the human body after long-term enrichment along with the cycle of matter and food
562 chain transmission, causing harm to human health (Dong, et al., 2021; Wright, et al., 2013).
563 Therefore, with the increasing demand for food safety, the "Fishery-PV Integration" aquaculture
564 mode will have broad development prospects. A Circos diagram can more intuitively show the
565 distribution of ARGs in each sample (Krzywinski, et al., 2009). In this study, five ARGs including
566 tetracycline resistance gene *tetH*, quinolone resistance gene *QnrVC6*, tetracycline resistance gene
567 *tetX*, tetracycline resistance gene *tet32*, and tetracycline resistance gene *tet34* appeared in shrimp
568 intestines, amount which tetracycline resistance gene *tetH* was the most abundant ARGs. Moreover,
569 macrolide resistance gene *MexL* and quinolone resistance gene *adeF* were the most abundant ARGs
570 in pond water and effluent. A previous study found ARGs in Antarctica and the Qinghai-Tibet
571 Plateau, both locations with little human activity (Chen, et al., 2016), suggesting that ARGs are
572 strongly transmissible in the environment (Wang , et al., 2018; Zhao , et al., 2018). In this study, 123
573 ARGs were detected without the use of antibiotics, which may be a result of ARGs from the
574 surrounding mariculture farms being transmitted and entered the mulching "Fishery-PV Integration"
575 aquaculture ponds through seawater. The occurrence of ARGs is correlated with the structure and
576 composition of the bacterial community (Guo, et al., 2017). Proteobacteria was the dominant phyla

of antibiotic resistance bacteria in all samples collected from the “Fishery-PV Integration” ponds. In addition, the proportion of Proteobacteria in shrimp intestines was larger than that in the whole microbial community, indicating that Proteobacteria carried more resistance genes than other phyla. Therefore, Proteobacteria may be a potential host of ARGs in the “Fishery-PV Integration” aquaculture environment.

5. Conclusions

Overall, “Fishery-PV Integration” farming features a stable micro-ecological environment. The microbiota ensures the healthy growth of shrimp by regulating the intestinal digestion and absorption of shrimp and preserving intestinal homeostasis; regulating the nitrogen transformation of the water body to ensure the stability of the water environment; and reducing the enrichment of ARGs in the shrimp to ensure food safety.

Acknowledgement

Our acknowledgement goes to all funders of this work.

Authors' contributions

All authors contributed experimental assistance and intellectual input to this study. The original concept was conceived by MZL, CBS, and XXL. Experimental strategies and sampling design were developed by MZL, XXL, and CBS. Sample collections, DNA extraction, DNA sequencing, and data analyses were performed by ZHH, JCZ, XYC and DWJZ. The manuscript was written by MZL, XXL, and CBS. The authors read and approved the final manuscript.

Funding

This research was funded by the key research and development projects in Guangdong Province (Grant No.2020B0202010009), the project of 2019 Annual Guangdong Provincial Special Financial Fund (Grant No.231419025), the project of the innovation team for the innovation and utilization of Economic Animal Germplasm in the South China Sea (Grant No.2021KCXTD026) and the Fangchenggang Science and Technology Plan Project (Grant No. AD19008017).

Availability of data and materials

The 16S rRNA gene sequencing datasets are available in the NCBI Sequence Read Archive (https://www.ncbi.nlm.nih.gov/sra) with the accession number SRP363824. The accession numbers of the metagenome sequencing is SRP367116.

Ethics approval and consent to participate

Not applicable.

Consent for publication

Not applicable.

Competing interests

The authors declare that they have no competing interests.

Authors' information

[1] College of Fisheries, Guangdong Ocean University, Zhanjiang, Guangdong, China.

[2] Guangdong Provincial Key Laboratory of Pathogenic Biology and Epidemiology for Aquatic Economic Animals, Zhanjiang, Guangdong, China.

[3] Guangdong Provincial Laboratory of Southern Marine Science and Engineering, Zhanjiang, Guangdong, China.

[†] These authors have contributed equally to this work.

[*] Correspondence: Chengbo Sun, suncb@gdou.edu.cn

References

Abriouel, H., Omar, N.B., Molinos, A.C., López, R., Ma, J.G., Martínez-Viedma, P., Ortega, E., CañAmero, M.M., Galvez, A., 2008. Comparative analysis of genetic diversity and incidence of virulence factors and antibiotic resistance among enterococcal populations from raw fruit and vegetable foods, water and soil, and clinical samples. International Journal of Food Microbiology. 123, 38-49.

Armstrong, A., Ostle, N.J., Whitaker, J., 2016. Solar park microclimate and vegetation management effects on grassland carbon cycling. Environmental Research Letters. 11, 074016.

Bahaidarah, H., Subhan, A., Gandhidasan, P., Rehman, S., 2013. Performance evaluation of a PV (photovoltaic) module by back surface water cooling for hot climatic conditions. Energy. 59, 445-453.

Bazilian, M., Onyeji, I., Liebreich, M., Macgill, I., Chase, J., Shah, J., Gielen, D., Arent, D., Landfear, D., Shi, Z., 2013. Re-considering the economics of photovoltaic power. Renewable Energy. 53, 329-338.

Blancheton, J.P., Attramadal, K.J.K., Michaud, L., d'Orbcastel, E.R., Vadstein, O., 2013. Insight into bacterial population in aquaculture systems and its implication. Aquacultural Engineering. 53, 30-39.

Buchfink, B., Xie, C., Huson, D.H., 2015. Fast and sensitive protein alignment using DIAMOND. Nature methods. 12, 59-60.

Chen, B., Yuan, K., Chen, X., Yang, Y., Zhang, T., Wang, Y., Luan, T., Zou, S., Li, X., 2016. Metagenomic analysis revealing antibiotic resistance genes (ARGs) and their genetic compartments in the Tibetan environment. Environmental science & technology. 50, 6670-6679.

638 Chen, J., Sharma, S., Quiocho, F.A., Davidson, A.L., 2001. Trapping the transition state of an ATP-binding cassette
639 transporter: evidence for a concerted mechanism of maltose transport. Proceedings of the National Academy of
640 Sciences. 98, 1525-1530.
641 Chen, X., He, Z., Zhao, J., Liao, M., Xue, Y., Zhou, J., Hoare, R., Monaghan, S.J., Wang, N., Pang, H., 2022.
642 Metagenomic Analysis of Bacterial Communities and Antibiotic Resistance Genes in *Penaeus monodon*
643 Biofloc-Based Aquaculture Environments. Frontiers in Marine Science.8
644 Cornejo-Granados, F., Lopez-Zavala, A.A., Gallardo-Becerra, L., Mendoza-Vargas, A., Sánchez, F., Vichido, R., Brieba,
645 L.G., Viana, M.T., Sotelo-Mundo, R.R., Ochoa-Leyva, A., 2017. Microbiome of Pacific Whiteleg shrimp
646 reveals differential bacterial community composition between Wild, Aquacultured and AHPND/EMS outbreak
647 conditions. Scientific reports. 7, 1-15.
648 Dickschat, J.S., 2010. Quorum sensing and bacterial biofilms. Natural product reports. 27, 343-369.
649 Dong, H., Chen, Y., Wang, J., Zhang, Y., Zhang, P., Li, X., Zou, J., Zhou, A., 2021. Interactions of microplastics and
650 antibiotic resistance genes and their effects on the aquaculture environments. Journal of Hazardous Materials.
651 403, 123961.
652 Dong, S.l., Dong, Y.w., Cao, L., Verreth, J., Olsen, Y., Liu, W.j., Fang, Q.z., Zhou, Y.g., Li, L., Li, J.y., 2022.
653 Optimization of aquaculture sustainability through ecological intensification in China. Reviews in Aquaculture.
654 Edgar, R.C., 2013. UPARSE: highly accurate OTU sequences from microbial amplicon reads. Nature methods. 10,
655 996-998.
656 Fändriks, L., 2017. Roles of the gut in the metabolic syndrome: an overview. Journal of internal medicine. 281,
657 319-336.

658 Fan, L., Wang, Z., Chen, M., Qu, Y., Li, J., Zhou, A., Xie, S., Zeng, F., Zou, J., 2019. Microbiota comparison of Pacific
659 white shrimp intestine and sediment at freshwater and marine cultured environment. Science of the Total
660 Environment. 657, 1194-1204.
661 Fang, H., Huang, K., Yu, J., Ding, C., Wang, Z., Zhao, C., Yuan, H., Wang, Z., Wang, S., Hu, J., 2019. Metagenomic
662 analysis of bacterial communities and antibiotic resistance genes in the *Eriocheir sinensis* freshwater
663 aquaculture environment. Chemosphere. 224, 202-211.
664 Feng, Q., Sun, Y., Wu, Y., Xue, Z., Cao, J., 2019. Physicochemical and Biological Effects on Activated Sludge
665 Performance and Activity Recovery of Damaged Sludge by Exposure to CeO2 Nanoparticles in Sequencing
666 Batch Reactors. International Journal of Environmental Research and Public Health. 16, 4029-.
667 Flegel, T.W., 2012. Historic emergence, impact and current status of shrimp pathogens in Asia. Journal of Invertebrate
668 Pathology. 110, 166-173.
669 Flieder, M., Buongiorno, J., Herbold, C.W., Hausmann, B., Rattei, T., Lloyd, K.G., Loy, A., Wasmund, K., 2021. Novel
670 taxa of Acidobacteriota implicated in seafloor sulfur cycling. The ISME journal. 15, 3159-3180.
671 Fu, L., Niu, B., Zhu, Z., Wu, S., Li, W., 2012. CD-HIT: accelerated for clustering the next-generation sequencing data.
672 Bioinformatics. 28, 3150-3152.
673 Gatesoupe, F.J., 1999. The use of probiotics in aquaculture. Aquaculture. 180, 147-165.
674 Giatsis, C., Sipkema, D., Smidt, H., Heilig, H., Benvenuti, G., Verreth, J., Verdegem, M., 2015. The impact of rearing
675 environment on the development of gut microbiota in tilapia larvae. Rep. 5, 18206.
676 Guo, J., Li, J., Chen, H., Bond, P.L., Yuan, Z., 2017. Metagenomic analysis reveals wastewater treatment plants as
677 hotspots of antibiotic resistance genes and mobile genetic elements. Water research. 123, 468-478.

HARGs-Moreno, J.M., Coutinho, F.H., Zaragoza-Solas, A., Picazo, A., Almagro-Moreno, S., Lopez-Perez, M., 2020. Dysbiosis in marine aquaculture revealed through microbiome analysis: reverse ecology for environmental sustainability. FEMS Microbiology Ecology. 96, fiaa218.

He, Z., Pan, L., Zhang, M., Zhang, M., Huang, F., Gao, S., 2020. Metagenomic comparison of structure and function of microbial community between water, effluent and shrimp intestine of higher place *Litopenaeus vannamei* ponds. Journal of Applied Microbiology. 129, 243-255.

Huang, F., Pan, L., Song, M., Tian, C., Gao, S., 2018b. Microbiota assemblages of water, sediment, and intestine and their associations with environmental factors and shrimp physiological health. Applied Microbiology and Biotechnology. 102, 8585-8598.

Huang, Z., Zeng, S., Xiong, J., Hou, D., He, J., 2020. Microecological Koch's postulates reveal that intestinal microbiota dysbiosis contributes to shrimp white feces syndrome. Microbiome. 8, 32.

Jia, B., Raphenya, A.R., Alcock, B., Waglechner, N., Guo, P., Tsang, K.K., Lago, B.A., Dave, B.M., Pereira, S., Sharma, A.N., 2016. CARD 2017: expansion and model-centric curation of the comprehensive antibiotic resistance database. Nucleic acids research, gkw1004.

Ju, Y., Li, C., Shen, P., Wu, X., Cao, L., Zhou, B., Yan, X., Pan, Y., 2021. Development of recombinase polymerase amplification combined with lateral flow detection assay for rapid and visual detection of *Ralstonia solanacearum* in tobacco. Plant Disease, PDIS-04-21-0688-RE.

Kanehisa, M., Goto, S., Sato, Y., Kawashima, M., Furumichi, M., Tanabe, M., 2014. Data, information, knowledge and principle: back to metabolism in KEGG. Nucleic acids research. 42, D199-D205.

Krzywinski, M., Schein, J., Birol, I., Connors, J., Gascoyne, R., Horsman, D., Jones, S.J., Marra, M.A., 2009. Circos: an information aesthetic for comparative genomics. Genome research. 19, 1639-1645.

LeBlanc, J.G., Chain, F., Martín, R., Bermúdez-Humarán, L.G., Courau, S., Langella, P., 2017. Beneficial effects on host energy metabolism of short-chain fatty acids and vitamins produced by commensal and probiotic bacteria. Microbial cell factories. 16, 1-10.

Li, D., Liu, C.-M., Luo, R., Sadakane, K., Lam, T.-W., 2015. MEGAHIT: an ultra-fast single-node solution for large and complex metagenomics assembly via succinct de Bruijn graph. Bioinformatics. 31, 1674-1676.

Lei (2006). Environmental Chemistry Experiment in Aquaculture Water. Beijing: China Agriculture Press 5-6, 56–70.

Li, J., Jia, H., Cai, X., Zhong, H., Feng, Q., Sunagawa, S., Arumugam, M., Kultima, J.R., Prifti, E., Nielsen, T., 2014. An integrated catalog of reference genes in the human gut microbiome. Nature biotechnology. 32, 834-841.

Li, L.-G., Huang, Q., Yin, X., Zhang, T., 2020a. Source tracking of antibiotic resistance genes in the environment—Challenges, progress, and prospects. Water Research. 185, 116127.

Li, P., Gao, X., Jiang, J., Yang, L., Li, Y., 2020b. Characteristic Analysis of Water Quality Variation and Fish Impact Study of Fish-Lighting Complementary Photovoltaic Power Station. Energies. 13, 4822.

Li, W., Godzik, A., 2006. Cd-hit: a fast program for clustering and comparing large sets of protein or nucleotide sequences. Bioinformatics. 22, 1658-1659.

Liu, J., Fu, X., Liu, J., 2017. Variation of physical and chemical factors in ponds of shrimp *Litopenaeus vannamei* with different cultural patterns. J. Guangdong Ocean Univ. 37, 113-117.

Liu, X., Steele, J.C., Meng, X.Z., 2017. Usage, residue, and human health risk of antibiotics in Chinese aquaculture: A review. Environmental Pollution. 223, 161-169.

Lucas, R., Courties, C., Herbland, A., Goulletquer, P., Marteau, A.L., Lemonnier, H., 2010. Eutrophication in a tropical pond: Understanding the bacterioplankton and phytoplankton dynamics during a vibriosis outbreak using flow cytometric analyses. Aquaculture. 310, 112-121.

720 Magoč, T., Salzberg, S.L., 2011. FLASH: fast length adjustment of short reads to improve genome assemblies.
721 Bioinformatics. 27, 2957-2963.
722 Martínez, J.L., Coque, T.M., Baquero, F., 2015. What is a resistance gene? Ranking risk in resistomes. Nature Reviews
723 Microbiology. 13, 116-123.
724 Nguyen, T.V., Ryan, L.W., Nocillado, J., Groumellec, M.L., Ventura, T., 2020. Transcriptomic changes across
725 vitellogenesis in the black tiger prawn (*Penaeus monodon*), neuropeptides and G protein-coupled receptors
726 repertoire curation. General and Comparative Endocrinology. 298, 113585.
727 Nielsen, H.B., Almeida, M., Juncker, A.S., Rasmussen, S., Li, J., Sunagawa, S., Plichta, D.R., Gautier, L., Pedersen,
728 A.G., Le Chatelier, E., 2014. Identification and assembly of genomes and genetic elements in complex
729 metagenomic samples without using reference genomes. Nature biotechnology. 32, 822-828.
730 Ondov, B.D., Bergman, N.H., Phillippy, A.M., 2011. Interactive metagenomic visualization in a Web browser. BMC
731 bioinformatics. 12, 1-10.
732 Orellana, L.H., Francis, T.B., FerrARGs, M., Hehemann, J.-H., Fuchs, B.M., Amann, R.I., 2021. *Verrucomicrobiota* are
733 specialist consumers of sulfated methyl pentoses during diatom blooms. The ISME Journal, 1-12.
734 Pringle, A.M., Handler, R., Pearce, J.M., 2017. Aquavoltaics: Synergies for dual use of water area for solar photovoltaic
735 electricity generation and aquaculture. Renewable and Sustainable Energy Reviews. 80, 572-584.
736 Pruden, A., Pei, R., Storteboom, H., Carlson, K., 2006. Antibiotic Resistance Genes as Emerging Contaminants: Studies
737 in Northern Colorado. Environmental Science & Technology. 40, 7445.
738 Quast, C., Pruesse, E., Yilmaz, P., Gerken, J., Schweer, T., Yarza, P., Peplies, J., Glöckner, F.O., 2012. The SILVA
739 ribosomal RNA gene database project: improved data processing and web-based tools. Nucleic acids research.
740 41, D590-D596.

741 Robert, Edgar, Brian, Haas, Jose, Clemente, Christopher, 2011. UCHIME improves sensitivity and speed of chimera
742 detection. Bioinformatics. 27, 2194–2200.
743 Rungrassamee, W., Klanchui, A., Maibunkaew, S., KARGsonuthaisiri, N., 2016. Bacterial dynamics in intestines of the
744 black tiger shrimp and the Pacific white shrimp during *Vibrio harveyi* exposure. Journal of invertebrate
745 pathology. 133, 12-19.
746 Schweinitzer, T., Josenhans, C., 2010. Bacterial energy taxis: a global strategy? Archives of Microbiology. 192,
747 507-520.
748 Segata, N., Izard, J., Waldron, L., Gevers, D., Miropolsky, L., Garrett, W.S., Huttenhower, C., 2011. Metagenomic
749 biomarker discovery and explanation. Genome biology. 12, 1-18.
750 Trapani, K., Redón Santafé, M., 2015. A review of floating photovoltaic installations: 2007–2013. Progress in
751 Photovoltaics: Research and Applications. 23, 524-532.
752 Urios, L., Michotey, V., Intertaglia, L., Lesongeur, F., Lebaron, P., 2008. *Nisaea denitrificans* gen. nov., sp. nov. and
753 *Nisaea nitritireducens* sp. nov., two novel members of the class *Alphaproteobacteria* from the Mediterranean.
754 International Journal of Systematic & Evolutionary Microbiology. 58, 2336-2341.
755 Valipour, M., 2012. Comparison of Surface Irrigation Simulation Models: Full Hydrodynamic, Zero Inertia, Kinematic
756 Wave. Journal of Agricultural Science. 4, 68-74.
757 Wang, J.-H., Lu, J., Zhang, Y.-X., Wu, J., Luo, Y., Liu, H., 2018. Metagenomic analysis of antibiotic resistance genes in
758 coastal industrial mariculture systems. Bioresource Technology. 253, 235-243.
759 Wang, L., Shao, Z., 2021. Aerobic Denitrification and Heterotrophic Sulfur Oxidation in the Genus *Halomonas*
760 Revealed by Six Novel Species Characterizations and Genome-Based Analysis. Frontiers in Microbiology. 12,
761 390.

762 Wang, Y., Wang, K., Huang, L., Dong, P., Zhang, D., 2020. Fine-scale succession patterns and assembly mechanisms of
763 bacterial community of *Litopenaeus vannamei* larvae across the developmental cycle. Microbiome. 8, 106.
764 Wma, B., A, W., My, A., Ms, A., Atw, C., 2020. Impact of dietary supplementation with *Eleutherine bulbosa* (Mill.) Urb.
765 on intestinal microbiota diversity and growth of white shrimp, *Litopenaeus vannamei* - ScienceDirect.
766 Aquaculture. 528.
767 Wright, S.L., Thompson, R.C., Galloway, T.S., 2013. The physical impacts of microplastics on marine organisms: a
768 review. Environmental pollution. 178, 483-492.
769 Xing, M., Hou, Z., Yuan, J., Liu, Y., Qu, Y., Liu, B., 2013. Taxonomic and functional metagenomic profiling of
770 gastrointestinal tract microbiome of the farmed adult turbot (Scophthalmus maximus). FEMS microbiology
771 ecology. 86, 432-443.
772 Xiong, J., Zhu, J., Dai, W., Dong, C., Qiu, Q., Li, C., 2017. Integrating gut microbiota immaturity and
773 disease-discriminatory taxa to diagnose the initiation and severity of shrimp disease. Environmental
774 microbiology. 19, 1490-1501.
775 Yannopoulos, S.I., Lyberatos, G., Theodossiou, N., Li, W., Valipour, M., Tamburrino, A., Angelakis, A.N., 2015.
776 Evolution of Water Lifting Devices (Pumps) over the Centuries Worldwide. Water. 7, 5031–5060.
777 Yuan, B., 2020. Observational Study on the Impact of Large-Scale Photovoltaic Development in Deserts on Local Air
778 Temperature and Humidity. Sustainability. 12. 3403
779 Zhang, C., Liang, Z., Hu, Z., 2014. Bacterial response to a continuous long-term exposure of silver nanoparticles at
780 sub-ppm silver concentrations in a membrane bioreactor activated sludge system. Water Research. 50, 350-358.
781 Zhang, M., Pan, L., Huang, F., Gao, S., Su, C., Zhang, M., He, Z., 2019. Metagenomic analysis of composition, function
782 and cycling processes of microbial community in water, sediment and effluent of *Litopenaeus vannamei*
783 farming environments under different culture modes. Aquaculture. 506, 280-293.

784 Zhao, Y., Zhang, X.-x., Zhao, Z., Duan, C., Chen, H., Wang, M., Ren, H., Yin, Y., Ye, L., 2018. Metagenomic analysis
785 revealed the prevalence of antibiotic resistance genes in the gut and living environment of freshwater shrimp.
786 Journal of hazardous materials. 350, 10-18.
787 Zhou, J., He, W.Y., Wang, W.N., Yang, C.W., Wang, L., Xin, Y., Wu, J., Cai, D.X., Liu, Y., Wang, A.L., 2009. Molecular
788 cloning and characterization of an ATP-binding cassette (ABC) transmembrane transporter from the white
789 shrimp *Litopenaeus vannamei*. Comparative Biochemistry & Physiology Toxicology & Pharmacology Cbp.
790 150, 450-458.
791 Zhu, L., Wu, Q., Dai, J., Zhang, S., Wei, F., 2011. Evidence of cellulose metabolism by the giant panda gut microbiome.
792 Proceedings of the National Academy of Sciences. 108, 17714-17719.